International Journal of Engineering Research and Technology. ISSN 0974-3154, Volume 13, Number 10 (2020), pp. 2742-2751
 https://dx.doi.org/10.37624/IJERT/13.10.2020.2742-2751

impact toughness, hardness in accordance with ASTM standards D638-02 , ISO 179-1: 2010/ 6110-04, D2583-07, D5023-01 and ASTM: D5418-01, respectively [22, 23, 24, 25]. Schematic drawings of the test specimens used with their dimensions are shown in Figure 1. Figure 2 (a & b) show the pouring of thoroughly mixed CSP and epoxy resin composite into a mould and the cured composite inside an enclosed glass mould, respectively.

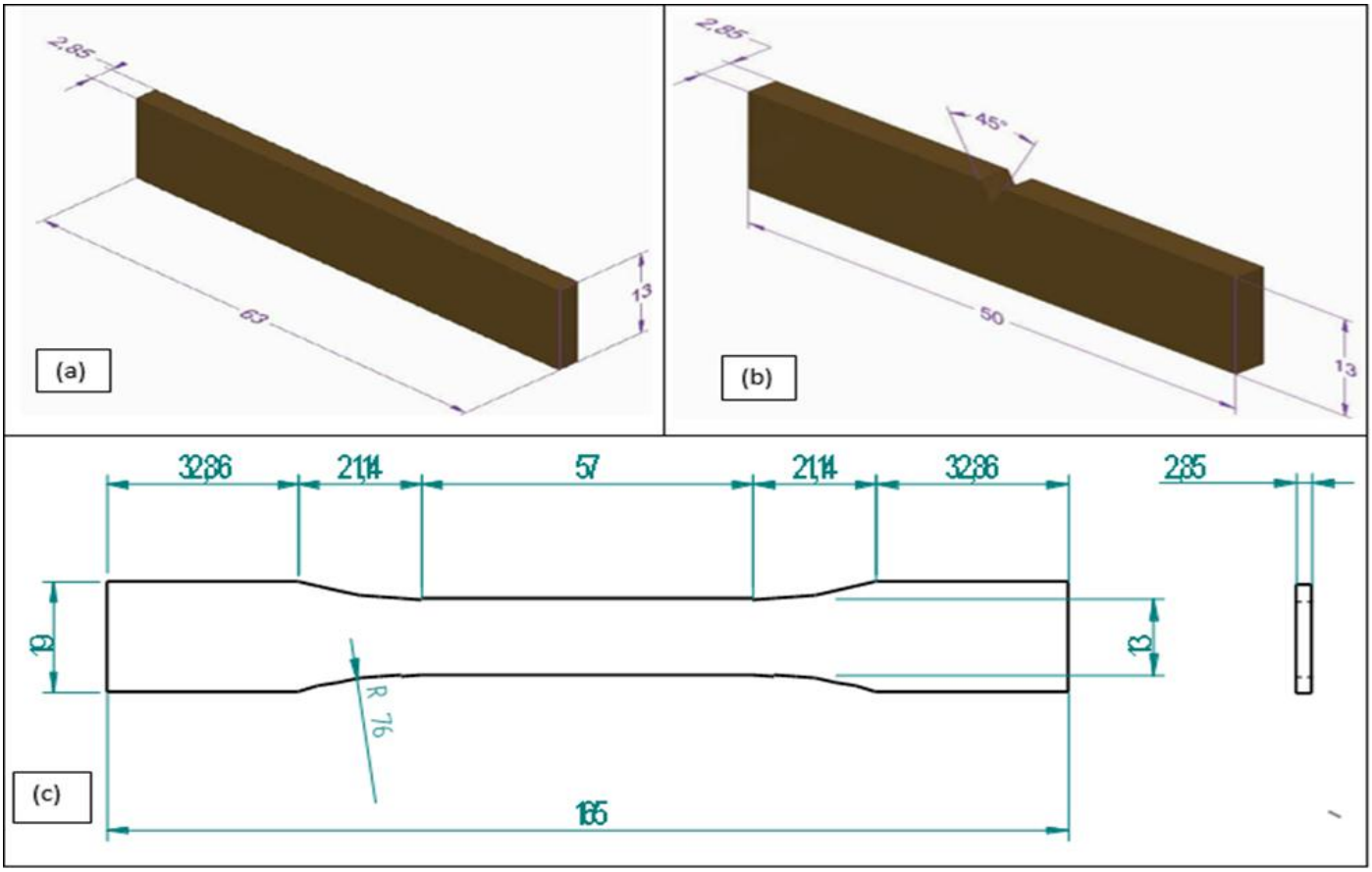

Figure 1: Schematic drawing (a) Hardness specimen according to ASTM D2583-07, (b) Charpy specimen according to ISO 179-1 and (c) Tensile specimen according to ASTM D638

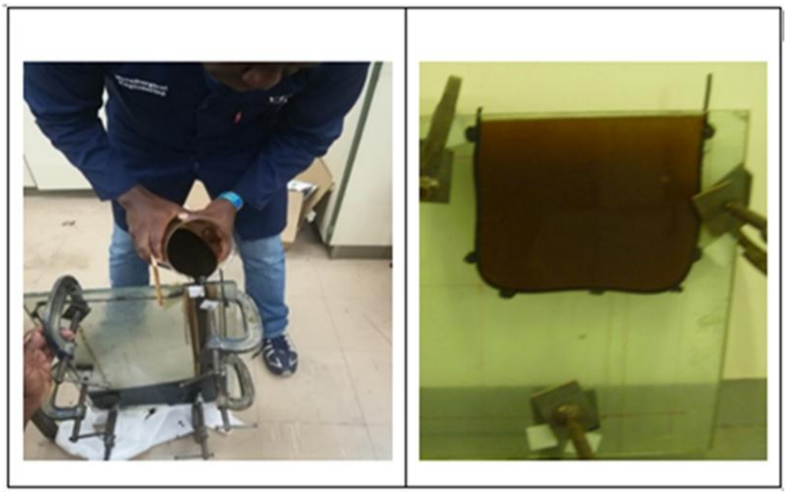

Figure 2: Pouring of the mixed reinforced coconut shell powder composite into the mould and the cast CSP epoxy resin/coconut particle composites

International Journal of Engineering Research and Technology. ISSN 0974-3154, Volume 13, Number 10 (2020), pp. 2742-2751
 https://dx.doi.org/10.37624/IJERT/13.10.2020.2742-2751

2.3 Mechanical testing

2.3.1 Tensile Testing

Dog-bone test specimens with a rectangular cross-section, prepared according to ASTM D638 as shown in Figure 3, were used for tensile testing.

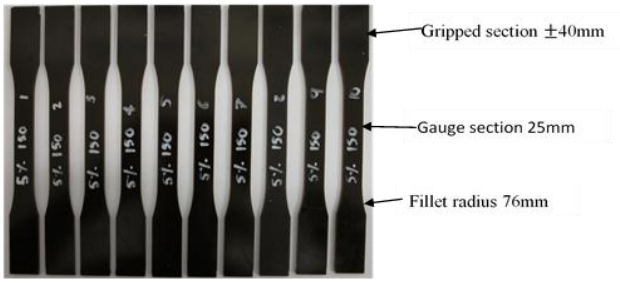

Figure 3: Dog bone tensile test specimens (ASTM D638)

Testing was performed with the Lloyd LR30k tensile testing machine shown in Figure 4 with a 30 kN load cell. The Epsilon extensometer with a gauge length of 25.00 mm and a maximum travel of 2.50 mm shown in the same Figure, was used to determine the extension of the specimen during the test. Ten identical specimens were tested, and average results calculated. All tensile testing was conducted at a room temperature of 23^{o}C and at a constant crosshead speed of 5 mm/min. Specimens of the dog-bone type shown in Figure 3 with a rectangular cross-section were used for testing.

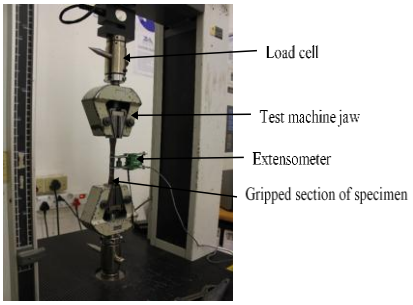

Figure 4: Lloyd LR30k tensile testing machine

Only 8 of the 10 specimens of 10% 150 µm that were tested failed within the gauge length as seem in Figure 5.

Figure 5: 10 weight percentage of 150 µm size CSP in epoxy resin composite specimens after tensile testing to failure

2.3.2 Charpy Impact Testing

The impact strength of specimens were determined according to the ISO 179-1: 2010/ ASTM 6110-04 test standards. Testing was performed utilising a Hounsfield Balanced Impact Machine. Test specimens were prepared according to ISO179-1: 2010/6110-04 ASTM, with a 45^{0} V-notch cut into the side each specimen as shown in Figure 1 (b). 10 identical specimens were used to determine the impact strength of composites for each type of composite.

2.3.3 Hardness Testing

The Barcol hardness of test specimens were determined according to ASTM: D2583-07. A Barber Colman – GYZJ 934-1 hardness impresser was first calibrated using the Colman calibration disks and then utilized for the test. For each composition, ten identical specimens were tested, and average results and standard deviation calculated.

3 RESULTS AND DISCUSSION

The results of tensile strength, tensile elastic modulus, percentage elongation, Charpy impact toughness and hardness of CSP/epoxy resin composites with different weight percentages of the CSP filler are presented in Figures 6-11, together with their accompanying discussions.

3.1 Tensile Strength and Elastic Modulus

Figure 6 shows the effect of CSP filler content (percentage weight) and particle size on the tensile strength of CSP/epoxy resin composites.

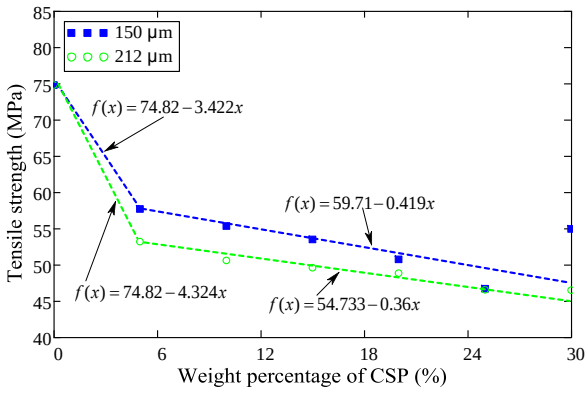

Figure 6: Tensile strength of CSP/epoxy resin composites versus weight percentage of the reinforcing CSP filler

The tensile strength of pure epoxy resin was determined as 75 MPa. It is clear from Figure 6 that for both the 150 µm and 212 µm filler particle epoxy resin composites, the effect of reinforcement was a continuous decrease of tensile strength with increasing addition of filler. For both filler particle sizes, two linear curves are evident in the figure, with initial steeper gradients up to a filler volume fraction of about 5wt%. The tensile strength of the composite is seen to be lower for the

International Journal of Engineering Research and Technology. ISSN 0974-3154, Volume 13, Number 10 (2020), pp. 2742-2751
 https://dx.doi.org/10.37624/IJERT/13.10.2020.2742-2751

larger size filler particles at all weight fractions of the reinforcing filler. Similar results were observed for groundnut shell particles reinforced epoxy composites [26] and for periwinkle shell particles reinforced polyester composites [27]. This decreasing trend is thought to be as a result of the weak interfacial bonding between the CSP filler and epoxy resin matrix due to increasing agglomeration with increasing filler weight fraction. Weak interfacial bonding leads to inefficient transfer of the stresses between the matrix and CSP filler thus giving rise to weaker composites [28]. Poor dispersion of the Nano fillers has been observed elsewhere to be the main factor that results in poor wetting and/or impregnation of reinforcing fibre, thus compromising mechanical strength, and is likely to be a contributing factor here as well [29, 30, 31].

The results of filler particle size and filler weight fraction on the elastic modulus of CSP/epoxy resin composites is shown in Figure 7.

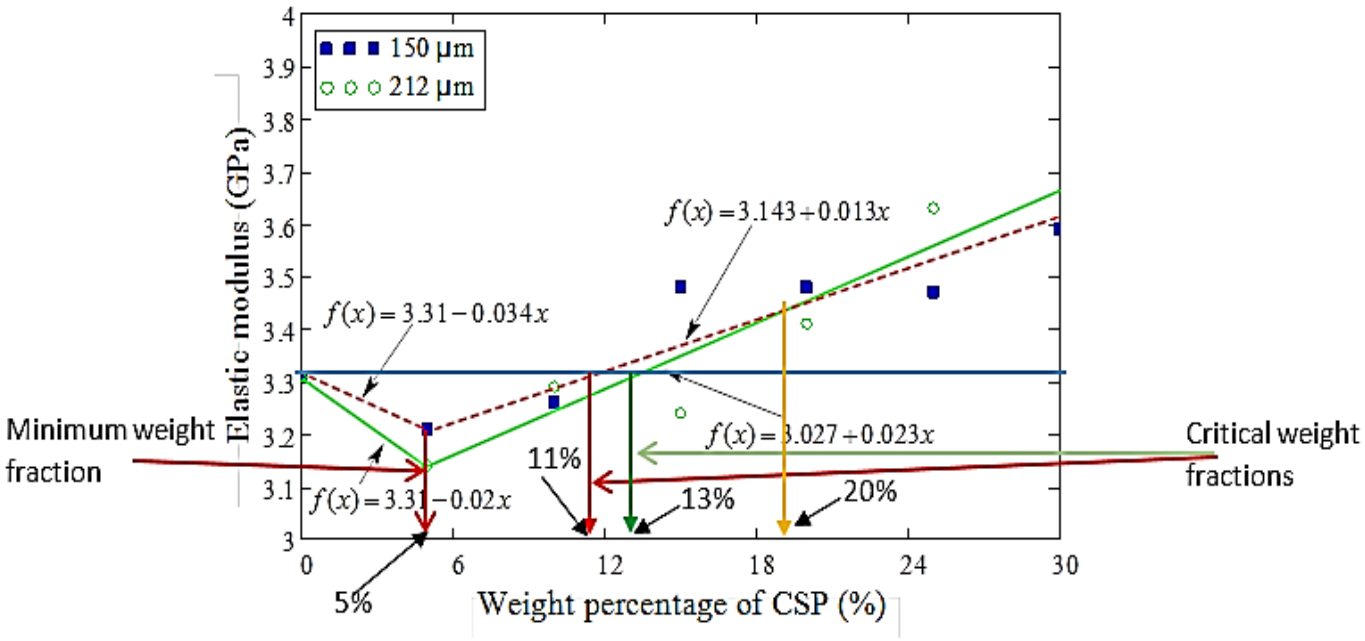

Figure 7: Elastic modulus of CSP/epoxy resin composites versus weight percentage of the reinforcing CSP filler

The Young modulus for the pure epoxy resin was determined as 3.31 GPa. Both curves in Figure 7 exhibit an initial decrease of Young modulus up till minimum values at a weight fraction of 5%. There was improvement in the Young modulus of the 150 µm CSP/epoxy resin composites over that of the pure epoxy resin above the critical weight fraction of 11wt%. The same applied to samples of 212 µm CSP/epoxy resin composites with a critical weight fraction of 13wt%. This shows that the introduction of coconut shell powder into epoxy resin matrix, leads to an initial decrease and an eventual increase in the magnitude of the elastic modulus of the CSP/epoxy resin composites. Both of these trends are consistent with standard theory of reinforcement. While the 150 µm CSP/epoxy resin filler composites had higher values of stiffness at lower weight fractions, the converse is true at higher weight fractions above 20wt%. This phenomenon may be as a result of poor interaction of the CSP with the epoxy resin with increasing filler contents of CSP.

In Figure 8 the percentage elongation to failure of CSP/epoxy resin reinforced composites are plotted for filler contents of 0,5,10,15,20,25, and 30% weight of 150 µm and 212 µm particle sizes of CSP.

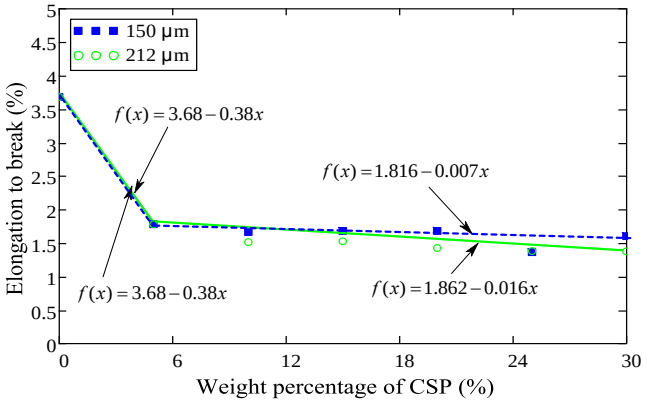

Figure 8: Percentage elongation of CSP/epoxy resin composites versus percentage weight CSP reinforcing filler

Figure 8 shows the percentage elongation to failure of the CSP/epoxy resin composites to decrease continuously with increasing content of CSP reinforcing filler for both filler particle sizes. The two curves both show a large initial drop in value between 0 and 5wt% for the CSP/epoxy resin composites of both 150 µm and 212 µm particles. This is followed by a gradual and continuous decrease of the percentage elongation

International Journal of Engineering Research and Technology. ISSN 0974-3154, Volume 13, Number 10 (2020), pp. 2742-2751
 https://dx.doi.org/10.37624/IJERT/13.10.2020.2742-2751

to failure with increasing weight fraction of the reinforcing CSP filler but at a lower rate. The decreasing trend was due to the higher rigidity of coconut shell-based nanoparticles than that of epoxy resin. The increase of filler reduces their mobility as result of crowding and therefore gives rise to an increase in brittleness of the filler reinforced composite. Another reason for the trend is that an increase of the content of filler leads to agglomeration of the filler particles instead of dispersion, which leads to weaker interfacial bonds and smaller surface areas for bonding. Coconut shell powder filler offers increased resistance to crack propagation in the composite [32]. As a result, there is a decrease of the percentage elongation of composites with CSP filler as compared to the neat epoxy resin. It is also noted that the percentage elongation of the lower particle size composites is lower at lower filler weight percentages and higher at higher filler weight percentages than the bigger particle size composites. This is likely to be a result of higher dispersion at lower volume fractions and less agglomeration at higher volume fractions, of the smaller than bigger particle size composites.

3.2 Charpy Impact Toughness

Figure 9 shows the Charpy impact toughness of CSP/epoxy resin reinforced composite for filler contents of 0,5,10,15,20,25, and 30% weight for 150 µm and 212 µm particle sizes of the CSP filler.

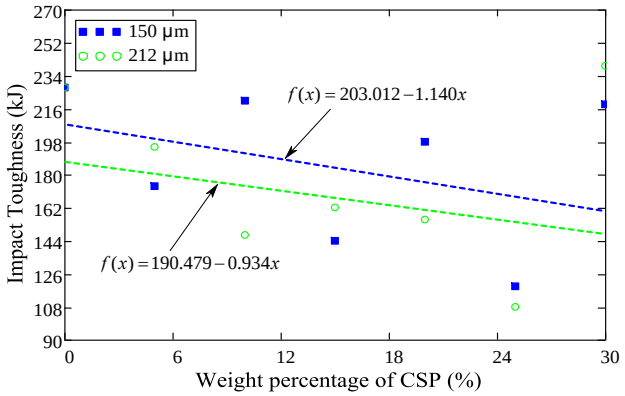

Figure 9: Charpy impact toughness versus weight percentage of CSP reinforcing filler versus weight percentage of filler

Though the values of Charpy impact toughness shown in Figure 9 exhibit a large scatter, there is a general declining trend of impact toughness with increasing percentage weight of CSP filler. This is as a result of lack of good adhesion between filler and matrix and less effective reinforcement both arising from increasing agglomeration with increasing filler weight percentage. The 150 µm CSP particle composites exhibit higher values of impact toughness compared to the 212 µm CSP particle composites. This trend is likely to be due to the fact that the smaller particles provide more crack arrest points for the same volume fraction and therefore enhance the toughness of the matrix more effectively.

Table 2 shows the values of Barcol hardness that were determined experimentally for epoxy resin, as well as, for both the CSP 150 µm and 212 µm particle size epoxy resin composites, for different weight fractions of CSP.

Table 2: Barcol hardness for 150 µm and 212 µm CSP particle size epoxy resin composites

Sample type	**Hardness (BHa)**
Neat epoxy resin	31.0 ± 2.11
5% 150 µm CSP/epoxy resin composites	36.0 ± 1.34
10% 150 µm CSP/epoxy resin composites	37.0 ± 1.43
15% 150 µm CSP/epoxy resin composites	41.0 ± 2.01
20% 150 µm CSP/epoxy resin composites	44.0 ± 0.94
25% 150 µm CSP/epoxy resin composites	46.0 ± 0.99
30% 150 µm CSP/epoxy resin composites	46.0 ± 1.72
5% 212 µm CSP/epoxy resin composites	36.0 ± 1.51
10% 212 µm CSP/epoxy resin composites	37.0 ± 1.17
15% 212 µm CSP/epoxy resin composites	41.0 ± 2.08
20% 212 µm CSP/epoxy resin composites	44.0 ± 1.25
25% 212 µm CSP/epoxy resin composites	46.0 ± 1.06
30% 212 µm CSP/epoxy resin composites	46.0 ± 2.27

Figure 10 shows the values of mean Barcol hardness of CSP/epoxy resin composites for CSP filler contents of 0%, 5%, 10%, 15%, 20%, 25% and 30% weight of 150 and 212 particle size of CSP, plotted against respective values of standard deviation

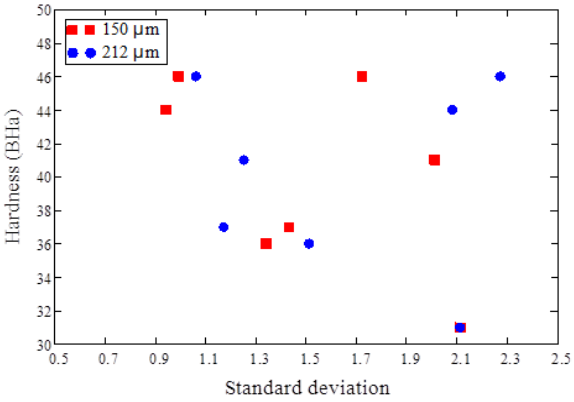

Figure 10: Values of mean Barcol hardness versus standard deviations for CSP/ epoxy resin composites for 150 µm and 212 µm CSP sizes.

International Journal of Engineering Research and Technology. ISSN 0974-3154, Volume 13, Number 10 (2020), pp. 2742-2751
 https://dx.doi.org/10.37624/IJERT/13.10.2020.2742-2751

A general trend emerges from the curves in Figure 10 of decreasing standard deviation with increasing mean Barcol hardness. This is expected as increasing hardness of the composite is a result of increased filler content, as is evident in the next figure, whose hardness is higher than that of the matrix.

Figure 11 shows the values of Barcol hardness results of CSP/epoxy resin composites for CSP filler contents of 0%, 5%, 10%, 15%, 20%, 25%, and 30% weight of 150 µm and 212 µm particle sizes of CSP, plotted against the weight fractions of filler.

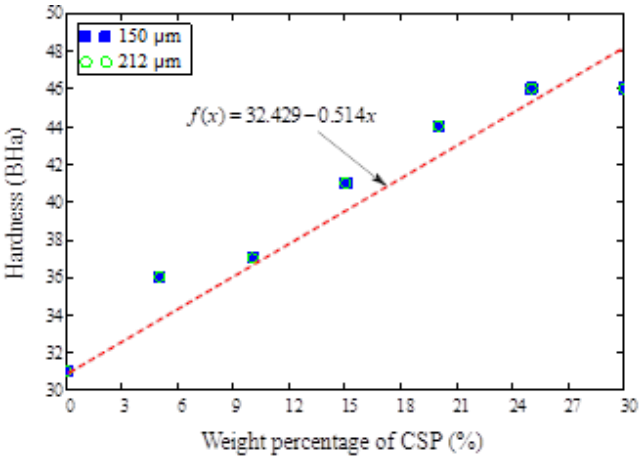

Figure 11: Effect of the percentage weight of CSP reinforcing filler on the hardness of CSP/ epoxy resin composites for 150 µm and 212 µm CSP sizes

It is evident from Figure 11 that, the hardness of CSP/epoxy resin composites increases continuously with increasing reinforcing filler's content for both the 150 µm and 212 µm CSP filler particles. The effect of reinforcing particle size is seen in the figure to be minimal as the two curves are more or less coincident at all weight fractions plotted.

3.4 Comparing Theoretical and Experimental Mechanical Properties of CSP/Epoxy Resin Composites

The particulate filler phase has been studied with reference to of weight fraction and particle sizes [27, 33]. It has been shown in research that for a given particulate volume fraction, the composite strength increases with decreasing particle size, and increasing volume fraction of the reinforcing filler [21, 27]. As a result, a variety of models are available to describe the modulus, tensile strength, and elongation at rapture as a function of filler volume fraction and particle sizes [33, 34]. The modulus and yield strength of particle-filled composites can be predicted from a number of models described by the Einstein equations, Guth and Smallwood model, Voigt rule Reuss model, and Kerner's equation, presented here as Equations 1 and 2, 3, 4 and 5, and from Nicolais-Narkis' equation presented here as Equations 6 and 8 [27, 34] . Expressions to predict the tensile strength of a particulate-filled composite from the UTS of the matrix (σ_m) and the volume fraction (V_p) of the reinforcing filler are presented here as Equations 1- 4 and 6-10. The equations show the strength of particulate-filled composites such as the coconut shell powder reinforced composite in the present study decreases with the increase in the percentage weight of reinforcing filler. Nielsen's equation, presented here as Equation 11, developed a basic model to describe the elongation of particulate composites at rapture, assumed perfect adhesion and therefore, fracture of the , polymer at the same elongation in the filled system as in the neat polymer [35].

$$E_C = E_m(1 + V_p) \quad (1)$$

$$E_c = E_m(1 + 2.5V_p) \quad (2)$$

$$E_c = E_m(1 + 2.5V_p + 14.1V_p^2) \quad (3)$$

$$E_c = E\_mv_m + E_pV_p \quad (4)$$

$$E_c = \frac{E_mE_P}{E_mV_p + E_pV_m} \quad (5)$$

$$\sigma_{yc} = \sigma_{ym}\left(1 - 1.21V_p^{2/3}\right) \quad (6)$$

$$\sigma_y = \sigma_m(1 - V_p) \quad (7)$$

$$\sigma_y = \sigma_{ym}(1 - 2.5V_p) \quad (8)$$

$$\sigma_c = \sigma_mV_m + \sigma_pV_p \quad (9)$$

$$\sigma_c = \frac{\sigma_m\sigma_P}{\sigma_mV_p + \sigma_pV_m} \quad (10)$$

$$\epsilon_c = \epsilon_m(1 - V_p^{1/2}) \quad (11)$$

Figure 12 shows both the experimental and predicted values of the tensile strength for CSP epoxy resin composites.

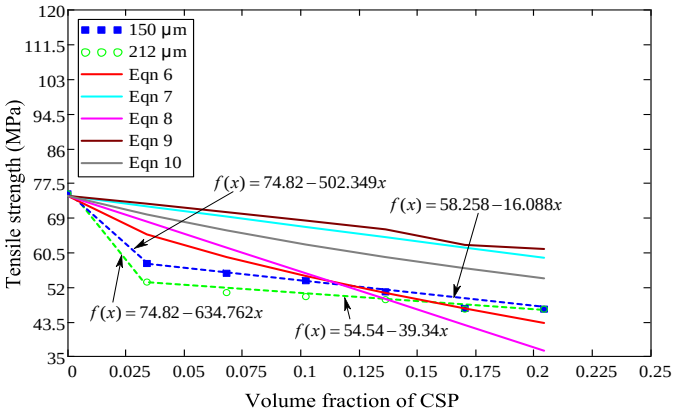

Figure 12: Comparison of experimental data with predicted data for tensile strength

International Journal of Engineering Research and Technology. ISSN 0974-3154, Volume 13, Number 10 (2020), pp. 2742-2751
 https://dx.doi.org/10.37624/IJERT/13.10.2020.2742-2751

The curves in Figure 12 show both the experimental and predicted values of the tensile strength to decrease with an increase in the volume fraction of the coconut shell powder. Both the experimental and results predicted from Equations 7, 8, 9 and 10 show linear decrease with the increasing volume fraction of the reinforcing filler, the former in two stages and the latter in a single stage. The results predicted from the theory of Nicolais-Narkis (Equation 6 and 8) are non-linear and linear, respectively, and are both closer to the experimental results, compared with those from Equations 7, 9 and 10, all which exhibit higher values than the experimental results. This shows that Equation 6 and 8 are best suited to predict the strength of this composite over the volume fraction range considered.

Experimental and theoretical curves of the variation in the magnitude of the modulus of elasticity of CSP reinforced epoxy composites for particle dimensions of 150 µm and 212 µm versus volume fraction are presented in Figure 13.

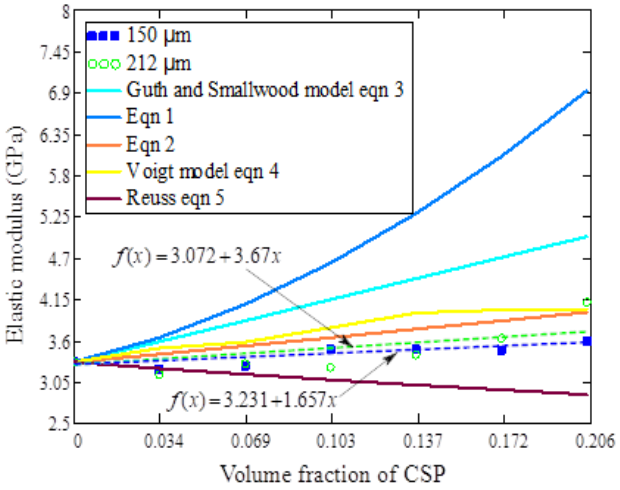

Figure 13: Comparison of experimental data with predicted data for elastic modulus

The experimental results presented in this Figure are compared with values calculated from the Einstein Equation's 1 and 2, Guth and Smallwood Equation 3 as well as the Voigt and Reuss Equations 4 and 5. The curves for Einstein's Equations 1 and 2, Guth and Smallwood Equation 3, and the Voigt rule exhibit values that are higher than the experimental results. The curve for Reuss model Equation 5 shows values that are less than the experimental values with a difference that increases with increasing volume fraction of the reinforcing filler in the range of volume fractions shown in the figure. This may be as a result of non-uniform spherical filler particle adhering well to the polymer matrix.

The curve for Guth and Smallwood Equation 3 exhibits values that are close to the experimental results with a difference that increases with increasing volume fraction of the reinforcing filler. Because it predicts reinforcement, Guth and Smallwood Equation 3 is best suited to predict the elastic modulus of the CSP/epoxy resin composite over the volume fraction of reinforcing filler investigated in this work.

Figure 14 shows a comparison of the experimental and theoretical values for percentage elongation for CSP epoxy resin composites

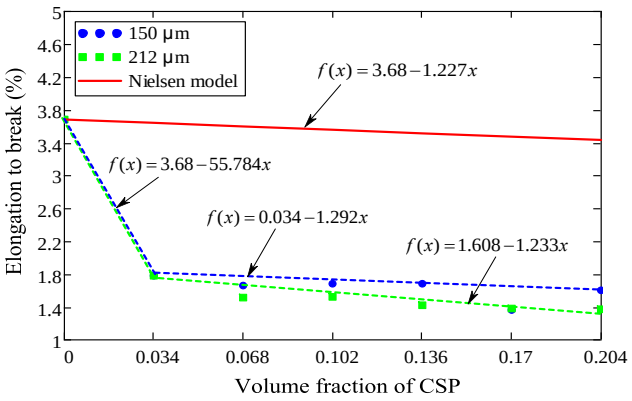

Figure 14: Comparison of experimental data with predicted data for elongation to rapture

The predicted values of percentage elongation from Nielsen's model Equation 11, decrease linearly with increasing volume fraction, the same as the experimental values. However, the latter shows two stage curves, with an initial steep gradient till a volume fraction of 0.34%. The experimental results are, however, much less than the predicted results. This may be as a result of poor adhesion that minimises the reinforcing effect of the fillers in comparison with the expectations based on theoretical models.

5.0 CONCLUSIONS

The following conclusions can be drawn from this work:

1) The mechanical properties of tensile strength, stiffness, percentage elongation, as well as toughness and hardness for CSP/epoxy resin composites are all affected by the size and content of CSP fillers.

2) The curves for stiffness exhibited the standard variations with weight fraction that are common to reinforced composites, complete with minimum and critical weight fractions. The larger particle sizes composites give rise to more effective reinforcement up to a weight fraction of 20% of the CSP filler and are less effective above this value.

3) Though a continuous reduction in the tensile strength and impact toughness of CSP/epoxy resin composites with increasing weight percentage of CSP filler particles of both sizes was observed, the effect was less for composites of the smaller particle size.

4) Coconut shell particle filled epoxy resin composites exhibited values of hardness that increased continuously with increasing percentage weight of CSP fillers and showed no discernible effect of filler particle size.

5) While the stiffness and hardness of CSP/epoxy resin composites showed an improvement on the values for raw epoxy resin, the former beyond a critical value of reinforcing filler volume fraction, the tensile strength, percentage elongation and toughness all decreased with the addition of CSP filler. The use of CSP as a reinforcing filler must therefore be for purposes of enhancing the first two mechanical properties, with the attendant reduction in the other three mechanical properties being taken on board

6) Different models were used to predict the mechanical properties of the CSP composites.

- The values of the tensile strength predicted by the Nicolais-Narkis theory (Equations 6 and 8) and by Equations 7, 9 and 10 showed decreasing trends of tensile strength with increasing weight fraction of the reinforcing filler with the curves for equations 6 and 8 fitted best to the experimental results.
- The values of the elastic moduli predicted by the Einstein Equations 1 and 2, Voigt Equation 4, and Guth and Smallwood Equation 3 showed values that were higher than the experimental results. The Reuss model Equation 5 exhibited values that were lower than the experimental results. Of all these models, Guth and Smallwood Equation 3 fitted best to the experimental results.
- The results of elongation to break that were predicted from Nielsen's Equation 11 were significantly different from the experimental results, possibly due to power interfacial adhesion between the filler particles and the matrix.

6.0 RECOMMENDATIONS

A study of a wider range of CSP particle sizes is recommended in order to determine trends and an optimum particle size.

CONFLICT OF INTEREST

The researchers have no conflict of interest to disclose with regard to the current research work.

ACKNOWLEDGEMENT

This research work was supported by the Vaal University of Technology (VUT), South Africa and Council for Scientific and Industrial Research (CSIR), South Africa.

REFERENCES

[1] Mohanty A. K., Misra M., and Drzal, L. T., J., 2002, Polymer Environment, Germany, pp. 10-19.

[2] RAO, M.D., 2003, "Recent applications of viscoelastic damping for noise control in automobiles and commercial airplanes". *Journal of Sound and Vibration*, 262(3), pp. 457-74.

[3] Neitzel, I., Mochalin, V., Koki, I., Palmese, G. R., and Gogotsi, Y., 2011, "Mechanical properties of epoxy composites with high contents of nanodiamond". Composite Science Technology, 71(5), pp. 710-6.

[4] Mohammed, L., Ansari, M.N.M., Pua, G., Jawaid, M., and Saiful Islam, M., 2015, "A review of natural fibre reinforced polymer. Composite and Its Application". International Journal of Polymer Science. Pp. 1-15.

[5] Kinoshita, H., Kaizu, K., Fukuda, M., Tokunaga, H., Keisuke Koga, K., and Ikeda, K., 2009, "Development of green composite consists of woodchips, bamboo fibres and biodegradable adhesive". Composite Part B: Engineering, Vol. 40, pp. 607-612.

[6] Khalil, H. P. S. A., Shahnaz, S. S., Ratnam, M. M., Ahmad, F., and Fuaad, N. N., 2006, "Recycle polypropylene (RPP) - wood saw dust (WSD) composites—Part 1: The effect of different filler size and filler loading on mechanical and water absorption properties". J. Reinf. Plast. Compos. 25(12), pp. 1291-13037.

[7] Dos Santos, L. P., Flores-Sahagun, T. S., and Satyanarayana, K. G., 2015, "Effect of processing parameters on the properties of polypropylene–sawdust composites". J. Compos. Mater. 49(30), pp. 3727-3.

[8] Sarki, J., Hassan, S. B., Aigbodion, V. S., and Oghenevweta, J. E., 2011, Potential of using coconut shell particle fillers in eco-composite materials. J. Alloys Compd. 509(5), pp. 2381-2385.

[9] Chun, K. S., Husseinsyah, S., and Azizi, F. N., 2013, "Characterization and properties of recycled polypropylene/ coconut shell powder composites": Effect of sodium dodecyl sulfate modification. Polym. Plast. Technol. Eng. 52(3), pp. 287-2.

[10] Kokta, B. V., Raj, R. G., and Daneault, C., 1989, "Use of wood flour as filler in polypropylene : Studies on mechanical properties". Polym. Plast. Technol. Eng. 28(3), pp. 247-259.

[11] Heckadka, S.S, Nayak, S.Y, Vikas, S.R., and Kini, M.V., 2016. "Investigation of tensile strength for areca frond/corn starch composites". *Indian Journal of Science,* 9(35).

[12] Frangopol, D.M., and Recek, S., 2003, "Reliability of fiber-reinforced composite laminate plates". Probabilistic Engineering Mechanics. Vol.18, pp. 119-137.

[13] Biswas, S., Kindo, S., and Patnaik, A., 2011, "Effect of length on coir fibre reinforced epoxy composites". Fiber and Polymers, Vol.12, pp. 73-78.

[14] Mohanty, A.K., Khan, M.A., and Hinrichen, G., 2000, "Surface medication of jute and its influence on performance of biodegradable jute-fabric/Biopol composites". Composite Science and Technology. 60(7), pp. 1115-1124.

[15] Mallick, P.K., 1993, "Fiber-Reinforced Composites". [Online]. Marcel Dekker: New York. Available at https://books.google.co.za/books/about/Fiber_Reinforced_Composites.html?id=z0MIzzOFMqkC&redir_esc=y. Accessed on the 13th of August 2016.

[16] Choi, S., and Sankar, B.V., 2008, "Gas permeability of various graphite/epoxy composite laminates for cryogenic storage systems". Part B, Vol.39, pp. 782-791. [Online]. Available at, http//www.sciencedirect.com. Accessed on the 12th of February 2017.

[17] Pervaiz, M., Panthapulakkal, S., Birat, K.C, Sain, M., and Tjong, J., 2016, "Emerging trends in automotive light-weighting through novel composite materials". Material Science and Application, Vol.7, pp. 26-38. [Online]. Available at, http://dx.doi.org/10.4236/msa.2016.71004. Accessed on the 12th September 2016.

[18] Verma, D., Cope, P.C., Shandilya, A., Gupta, A., and Maheshwari M.K., 2013, "Coir fibre reinforcement and application In polymer composite": A review. Journal of Material Environment Science, 4(2), pp. 263-276.

[19] Okubo, K., Fujii, T., and Yamamoto, Y., 2004, "Development of bamboo-based polymer composites and their mechanical properties". Composites Part A: Applied Science and Manufacturing, 35(3), pp. 377-383.

[20] Kumar, P. A, Mohamed, M. N, Philips, K.K., and Ashwin, J., 2016, "Development of novel natural composites with fly ash reinforcements and investigation of their tensile properties". Applied Mechanics and Materials, Vol. 852, pp. 55-60. [Online] Available at, https://www.researchgate.net/publication/307881349_Development_of_Novel_Natural_Composites_with_Fly_Ash_Reinforcements_and_Investigation_of_their_Tensile_Properties. Accessed on the 12th October 2016.

[21] Nawang, R., Danjaji, I., Ishiaku, U., Ismail, H., and Mohd Ishak, Z., 2001, "Mechanical properties of sago starch-filled linear low-density polyethylene (LLDPE) composites", Polymer Testing, 20(2), pp. 167-172.

[22] Standard Test Method for Tensile Properties of Plastics D638M- 87b, Annual Book of ASTM Standard, Volume 08.01 Plastics (I): D 256 - D 3159, 1988.

[23] Standard Test Method for Unnotched Cantilever Beam Impact Resistance of Plastics, Designation: D 4812 – 99, Annual Book of ASTM Standard, Volume 08.02 Plastics (II): D 3222 - D 5083, 2007.

[24] Standard Test Method for Indentation Hardness of Rigid Plastics by Means of a Barcol Impressor, Designation: Annual Book of ASTM Standard, D 2583 – 07, Annual Book of ASTM Standard, Volume 08.01 Plastics (I): D256-D 3159(2007).

[25] Standard Test Method for Plastics: Dynamic Mechanical Properties: In Flexure (Three Point Bending), Designation: Annual Book of ASTM Standard, D 5023 – 01, Annual Book of ASTM Standard, Volume 08.02 Plastics (I): D256-D 3159(2001).

[26] Raju, G.U., and Kumarappa, S., 2011, "Experimental study on mechanical properties of groundnut shell particle reinforced epoxy composites". *Journal of Reinforced Plastics and Composites*, Vol.30, pp. 1029-1037.

[27] Njoku, R.E., Okon, A.E., and Ikpaki, T.C., 2011, "Effects of variation of particle size and weight fraction on the tensile strength and modulus of periwinkle shell reinforced polyester composite", *Nigerian J. Technol*. Vol. 30, pp. 87-93.

[28] Ma, P. C., and Kim, J. K., 2011, "Carbon Nanotubes for Polymer Reinforcement", CRC Press, Boca Raton, FL, USA.Doi: 10.4028/www.scientific.net/AMR.879.90.

[29] Ajayan, P. M., Suhr, J., and Koratkar, N., 2006, "Utilizing interfaces in carbon nanotube reinforced polymer composites for structural damping". *Journal of Materials Science* 41(23), pp. 7824-7829. DOI: 10.1007/s10853-006-0693-4.

[30] Tarfaoui, M., Lafdi, K., and El Moumen, A., 2016, "Mechanical properties of carbon nanotubes-based polymer composites," Composites Part B: Engineering 103:113- 121. DOI: 10.1016/j.compositesb.2016.08.016.

[31] Tehrani, M., Boroujeni, A. Y., Hartman, T. B., Haugh, T. P., Case, S. W., and Al-Haik, M. S., 2013, "Mechanical characterization and impact damage assessment of a woven carbon fiber reinforced carbon nanotube-epoxy composite," Composites Science and Technology Vol. 75, pp. 42-48. DOI: 10.1016/j.compscitech.2012.12.005

[32] Islam, M.D, Das, S., Saha, J., Paul, D., Islam, M., Rahman, M., and Khan, M., 2017, "Effect of Coconut Shell Powder as Filler on the Mechanical Properties of Coir-polyester Composites". Chemical and Materials Engineering. Vol.5, pp. 75-82. 10.13189/cme.2017.050401.

[33] Fu, S.Y., Feng, X.Q., Lauke, B., and Mai, Y.W. 2008, "Effects of particle size, particle/matrix interfacing adhesion and particle loading on mechanical properties of particulate-polymer composites". Composite: Part B,39:933-961.

[34] Bourkas, G., Prassianakis, I., Kytopoulos, V., Sideridis, E., and Younis, C., 2010, "Estimation of elastic moduli of particulate composites by new models and comparison with moduli measured by tension, dynamic, and ultrasonic tests". Advances in Materials Science and Engineering, 13 doi:10.1155/2010/891824

[35] Kaully, T., Siegmann, A., and Shacham, D., 2008, "Mechanical behaviour of highly filled natural CaCO3 composites: effect of particle size distribution and interface interactions". Polymer composites, 29(4), pp. 396-408.